Decorrelation of the Light-emitting-Diode Internal-quantum-Efficiency Components

Studies of the Electron-hole Concentration-ratio at the Active-region Edge

Dinh Chuong Nguyen[1,2], David Vaufrey[1,2] and Mathieu Leroux[3]

[1]*Univ. Grenoble Alpes, F-38000, Grenoble, France*

[2]*CEA, LETI, MINATEC Campus, F-38054, Grenoble, France*

[3]*CNRS – Centre de recherche sur l'Hétéro-Epitaxie et ses Applications (CRHEA), Rue Bernard Grégory, 06560, Valbonne, France*

1 RESEARCH PROBLEM

GaN-based light-emitting diodes (LEDs) have strongly emerged, especially since the last decade, as a very promising white-light source, enabling them to enter many lighting applications and even further. Those applications mostly required the LEDs to function at a high-current regime. However, LEDs still suffer a critical internal-quantum-efficiency (IQE) loss, known as "droop". Their IQE falls drastically at high current-injection after reaching a peak value at usually relatively low current-densities (Krames et al., 2007; Morkoç, 2008), degrading the radiative-recombination rate and the output power (Cabalu et al., 2006; M.-H. Kim et al., 2007), a behavior that can be described as a sublinear increase in light-emission intensity with increasing diode current-density. The efficiency droop was first observed in GaN-based LEDs by (Krames et al., 2000) and (Mukai et al., 1999). The loss' main mechanism still remains an important topic that has raised intense debate by many reasons.

First, the knowledge about the wurtzite GaN is not complete as several parameters still suffer from uncertainty, such as the recombination coefficients or the carrier mobility. The Auger-recombination coefficients obtained from numerical calculations and curve-fitting can largely differ from each other, even though it is related to one of the widely-accepted droop-inducing processes. The carrier-mobility variation in GaN is noticed to be different from that in the well-understood Si, yet only one model for electron mobility was proposed (Turin, 2005).

Second, though theoretically explained, the internal mechanisms, especially the recombination, cannot be separately evaluated by characterization, or at least in an easy way. Their discrimination is critical as they can replace each other as the main loss-inducing mechanism in respect to the LED functioning-regimes. It has been attempted several times but the results are still under discussion.

The aforementioned difficulties hinder the droop reducing but the research activities are still ongoing. However, in addition to the applied methods, it may be suggested that new approaches be proposed.

2 OUTLINE OF OBJECTIVES

The LED efficiency-loss being complicated and involving many different mechanisms that cannot be easily and separately studied, this PhD. thesis thus aims to contribute to the decorrelation of these different droop-inducing factors. It mainly focuses on the ratio between the electron and hole concentrations that are injected into the active region of an LED and contribute to light emission. Nonetheless, other non-radiative recombination processes are also taken into account.

This work consists in two parts: LED modeling and characterizing. The samples are mostly commercial LEDs but can also be provided by internal research-projects. Initially, the modeling is expected to provide an insight into the LED internal-mechanisms in order to evaluate the impact of each mechanism on the efficiency loss. The understanding of those impacts' degree could help design a more innovative LED structure in which the mechanisms favorable to the LED lighting-function are intensified and the loss-inducing ones are reduced. The characterization allows to verify the hypothesis deduced from the simulation.

However, a simulation can also be carried out based on characterization results since the efficiency on several internal-project-LEDs can show a strong improvement without its reasons being clearly explained.

Nguyen D., Vaufrey D. and Leroux M..
Decorrelation of the Light-emitting-Diode Internal-quantum-Efficiency Components - Studies of the Electron-hole Concentration-ratio at the Active-region Edge.
Copyright © 2015 SCITEPRESS (Science and Technology Publications, Lda.)

Based on the acquired knowledge from modeling and characterization, as stated above, more-innovative high-power LED structures are expected to be designed.

3 STATE OF THE ART

Many groups have proposed different mechanisms that they judge to be the main reason of the LED droop. Those mechanisms are very diverse but as until 2014, two mainstream processes remain most relevant to the IQE droop.

On the one hand, (Hader et al., 2008) have simulated the magnitude of direct Auger-recombination in the (AlGaIn)N material system and concluded that Auger losses are too small to account for the droop. Meanwhile, by taking phonon-assisted Auger-recombination into account, (Kioupakis et al., 2011) were able to obtain higher Auger-coefficient values which are in good agreement with the experiments (Galler et al., 2012). (Delaney et al., 2009) have computed the Auger coefficient by the first-principles density-functional and reported values that can be as large as $2 \times 10^{-30}\,\mathrm{cm}^6\mathrm{s}^{-1}$ when the bandgap is approximately 2.5 eV, enabling the Auger processes to be the main cause of the droop. However, this coefficient is significantly reduced as the band gap is higher or lower than 2.5 eV. (Iveland et al., 2013) have gone further by directly measuring the Auger-induced electrons from an LED under electrical injection and concluded that the Auger processes are the origin of the droop phenomenon. Comments upon their results were given by (Bertazzi et al., 2013).

On the other hand, by comparing the optical and electrical properties of AlGaInN-barrier-enhanced LEDs with those of GaN-barrier-enhanced LEDs, (Schubert et al., 2008) suggested that carrier leakage might be the dominant cause of the efficiency droop. Through experiments and simulation of the polarization-field-enhanced carrier-leakage, (M.-H. Kim et al., 2007) also strengthened this assumption. Other works based on electron leakage enhanced by high internal piezoelectric fields were published elsewhere (Rozhansky and Zakheim, 2007; Schubert et al., 2007; Xu et al., 2009). It was also suggested that poor hole-injection may reduce the efficiency (David et al., 2008; Ni et al., 2008; Zhang et al., 2014).

Apart from these two main schools of thought, several groups have indicated other different mechanisms that may lead to the LED efficiency-droop, including recombination at dislocation (Hangleiter et al., 2005), self-heating as the current increases (Cao and Arthur, 2004). Recently, (Huang et al., 2013) reported the effect of the lateral current-spreading on the efficiency droop in a conventional-chip LED. Studies on current spreading in vertical LEDs were also carried out (Li and Wu, 2012; Son et al., 2012). In this paper, the mentioned samples and simulation models are both vertical-thin-film (VTF) LEDs. A VTF LED structure is flipped from the conventional epitaxial stack, with an n-type layer under a p-type layer and the cathode facing the anode. The experimental results and the corresponding simulations will be reported and show that the efficiency droop in VTF GaN-based LEDs is partly tuned by spreading.

4 METHODOLOGY

As the semiconductor-device simulation is mainly numerical, the initial approach is to build a model for GaN-based LEDs by analytically solving the mathematical expressions. These expressions are interconnected and solving them involves the use of special functions; hence analytical solutions can hardly be obtained.

Another approach was then carried out. Since the current passing through an LED mainly consists in electrons due to their low effective-mass and high mobility, while the amount of emitted-light is tuned by the holes as they are minority carriers, the electroluminescence characterization can provide an estimation of the ratio between these carriers. Furthermore, through pulsed-electroluminescence characterizations, their injection efficiencies can be evaluated due to the difference in mobility. Consequently, a pulsed-electroluminescence setup was realized. The recorded data were later processed and compared to the simulation results in a following communication.

As for the modeling, the ATLAS package from SILVACO Corporation is utilized. The carrier concentration is calculated with special attention, especially at the edges of the active region, because their enhancing or limiting role will become clear at these positions. The simulation can be coupled with characterization whether to verify the modeling accuracy or to explain the measurements. The work presented later in this paper was based on the characterization results from two different LED-structures. The simulation was later carried out to partly explain the observed changes between the two structures. Deeper studies on the carrier concentrations followed and provided an insight into

the unbalanced distributions of electrons and holes entering the active region, where they might eventually recombine. This observation then suggested that the p-type layer play an important role in the carrier transport and lead to the p-GaN-properties studies through characterization.

5 EXPECTED OUTCOME

The electroluminescence measurements show a time shift between the onset of the current signal and that of the luminous signal. This shift is expected to represent the different degrees of carrier-injection efficiency if it varies with regard to the material parameters. The data processing was still ongoing when this article was being written.

The studies on the p-GaN properties could provide additional information needed to better understand the carrier behaviors and their impact on the efficiency loss. They can help complete the modeling and eventually establish the ratio between the electron and the hole concentrations, hence this ratio's weight in the IQE droop can hopefully be estimated. Sample preparations are expected to be finished shortly.

If these goals are achieved, by the end of this PhD. thesis, new ideas for a more efficient LED-design might be proposed.

6 STAGE OF THE RESEARCH

In this paper, the work carried out through modeling will be presented. Its results will be applied in the incoming works.

This work started from the characterization results obtained on a project's samples, followed by the ATLAS software package simulation.

6.1 Sample Structure and Simulation Model

Two sample structures were fabricated, electrically and optically characterized. Those are square 900 µm × 900 µm LEDs, differing from each other only in their cathode. The first structure, hereby called LED 1, has a round 100-µm-diameter cathode, situated in the middle of its surface. The second structure, LED 2, has multiple-stripe-like cathodes that are parallel to each other. These two structures were modeled as described below with the same parameters. Though the structure used to model the LED 1 does not possess a round cathode, its section should resemble that of the LED 1.

To simulate the aforementioned LED 1 and LED 2, two vertical GaN-based LED structures with different-shaped cathodes are modeled: the LED A has a single-striped cathode that is placed in the middle of the p-type surface, while the LED B has nine striped-cathodes that are parallel to each other. Their widths are also 900 µm. In the LED A, the cathode width is set to 225 µm. The cathodes in the LED B are 25 µm-wide and separated from each other at a distance of 75 µm. Consequently, in both structures, the total area covered by the cathodes is equivalent. The p-type layer is 3-µm-thick and the ionized-acceptor concentration is 5×10^{17} cm^{-3}. The n-type-layer thickness and ionized-donor concentration are respectively kept at 3 µm and 5×10^{18} cm^{-3}. All the doping profiles are uniform. Both structures also consist of five 3-nm-thick undoped $In_{0.1}Ga_{0.9}N$ quantum wells, separated by four 10-nm-thick GaN barriers. However, neither of them consists of an electron-blocking layer (EBL). The anode covers the full surface of the LED structures. Both the anode and cathode are considered to be ohmic contacts. The section of one-half of the LED A is shown in Figure 1(a) and the section of one-third of the LED B is shown in Figure 1(b). Note that they are not in exact scale.

As stated before, the simulations were carried out on the ATLAS software package by SILVACO Corporation. Standard Shockley-Read-Hall (SRH), Auger and three-band radiative-recombination models are used to respectively simulate the non-radiative and radiative mechanisms. For the SRH model, the electron and hole lifetimes are both fixed at 100 ns. This value is high compared to those reported in the state of the art but approximate to those reported by (Delaney et al., 2009) and will reduce the SRH-recombination rate. Meanwhile, the trap energy level for this recombination is situated in the middle of the band gap, meaning that the highest possible SRH-recombination rate is computed. The electron and hole Auger-coefficients are set to be 10^{-30} cm^{6}s^{-1}, a larger value than the usually reported ones in the state of the art in order to enhance Auger recombination. The built-in electric charges occurring at the p-n interface due to spontaneous and piezoelectric polarization were also calculated. Its theoretical value is usually reduced due to screening effects, but the extent of this reduction is still uncertain (Della Sala et al., 1999; Piprek et al., 2006; Romanowski et al., 2010). Hence, in our simulation, the final polarization charge density is assumed to be 80% of the theoretical value. The defect-related loss

was not taken into account during the simulation and the temperature is kept at 300 K.

Several other assumptions were made to simplify the simulations. The electron and hole mobility are respectively 400 cm^2/Vs and 8 cm^2/Vs. However, in the InGaN quantum wells, they are both 100 cm^2/Vs. All these values are suggested by ATLAS. They are kept constant throughout the simulation for two main reasons. The first one is to lighten the model. The second one is the lack of empirical models for electron and hole mobility, especially under the effect of a high electric field, except the model proposed by (Turin, 2005). That being said, at high injection currents, the modeled LED-behaviors will deviate from the common experimental characteristics.

In order to simulate the light output, the radiative-recombination rate is only integrated over the areas that are not shaded by the cathodes.

6.2 Experimental Results

The experimental results obtained on a set of samples are plotted in Figure 2. It can be clearly seen in Figure 2(a) that the IQE and especially its peak-value are higher in the LED 2 than in the LED 1. Moreover the current density corresponding to this peak value is also higher in the LED 2 than in the LED 1, shifted to approximatively 15 A/cm^2 instead of 10 A/cm^2.

Furthermore, Figure 2(b) displays the normalized IQE from the two LEDs. The droop is more significant in the LED 1 than in the LED 2, with efficiency falling to less than 40 % of the peak value at 100 A/cm^2. The forward-current density and the optical-power density of the LED 2 also respectively exceed those of the LED 1, as shown on Figure 2(c) and Figure 2(d). These results imply that by replacing a round cathode by a multiple-arrayed cathode, the LED performance can be critically enhanced and the droop reduced. To further understand this difference, the next sections will discuss the simulation results for the LEDs A and B which are representative for the LEDs 1 and 2, respectively.

6.3 Studies by Modeling

6.3.1 Current-spreading Analysis

Due to the multiple-stripe-like cathode-geometry, current spreading certainly occurs in the LED structure. The current spreading length was shown to depend on the forward voltage and for GaN-based LEDs, the Thompson spreading-current model was demonstrated to be more appropriate than the Guo-Schubert model (H. Kim et al., 2007). Since the stripe-like electrodes in our experiments are located on a thick n-type layer, the current is more likely to totally spread throughout the n-type layer before entering the p-type layer. Thus, the current-spreading is mainly considered to occur in the n-layer and its length was calculated for the two LEDs A and B by the Thompson model (Thompson, 1980)

$$L_s = \sqrt{\frac{nk_BTt_n}{q\rho_nJ_0}} \quad (1)$$

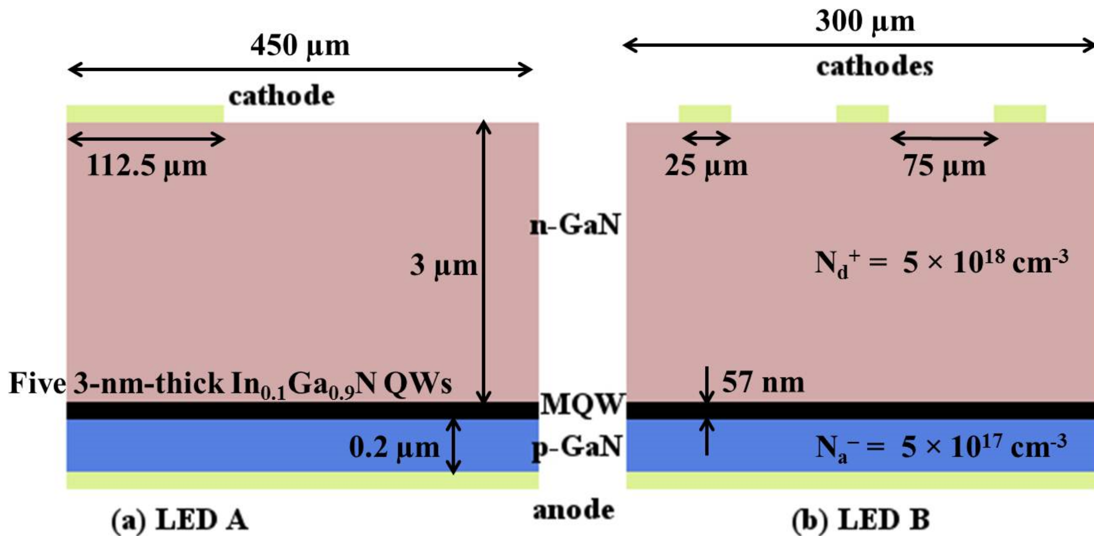

Figure 1: (a) One-half of the LED A; (b) One-third of the LED B with three cathodes. The material parameters are the same in both structures; hence they are displayed in only one of the structures.

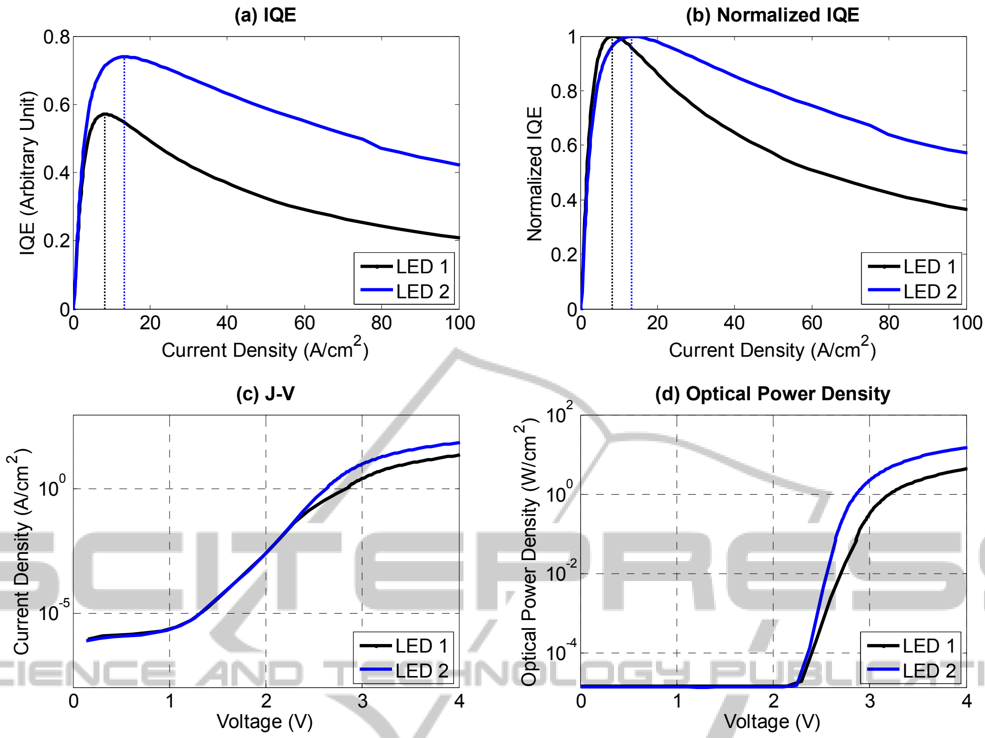

Figure 2: The experimental results from the LED 1 (black solid line) and the LED 2 (blue solid line), respectively a) Efficiency, b) Normalized efficiency, c) J-V characteristic curve and d) L-V curve.

where n, k_B, T, t_n, q, ρ_n are respectively the ideality factor, the Boltzmann constant, the temperature, the n-layer thickness, the elementary charge and the n-layer resistivity. J_0 is the current density at the edge of the contact. The current density J(x) extending away from the contact is given by

$$J(x) = \frac{2J_0}{(x/L_s + 2)^2} \quad (2)$$

J_0 can be approximated as the uniform current-density under the cathodes, which can be measured from the simulation. The n-type layer resistivity was approximated by $\rho_n = (N_d q \mu_n)^{-1}$ and the ideality factor was extracted from the simulated J-V curve as $n = (qJ_0)/(k_B T) \times (\partial V/\partial J_0)$. Included in the equation **Error! Reference source not found.**, this gives

$$L_s = \sqrt{t_n N_d \mu_n q \times (\partial V/\partial J_0)} \quad (3)$$

An integral of the equation (2) from the edge of the contact to a position t gives

$$\int_0^t J = 2J_0 L_s \left[\frac{1}{\sqrt{2}} - \frac{1}{t/L_s + \sqrt{2}}\right] \quad (4)$$

which represents the electric-current intensity per unit length covering from the contact edge to the position t. By multiplying it by the number of the unshaded areas in the LEDs A and B, one obtains the current intensity per unit length in the whole part of the LED where light extraction is not hindered by the opaque cathodes. The formula (4) also suggests that a higher current-injection is more likely achieved when the distance t is lower than L_s.

The calculations indeed indicate that the LED B with the multiple-striped cathodes injects a higher current intensity than the LED A with the single-striped cathode. However, this information still cannot fully explain the shift of the IQE peak and the IQE increase. As shown by Figure 3, the IQE of the LED B at a certain current density can remain higher than that of the LED A at a lower current density while intuitively the IQE should decrease as the current density increases. An insight into the IQE is then needed and presented in the next section.

6.3.2 Internal-quantum-Efficiency and Carrier-concentration Profile

Figure 3 shows the calculated internal quantum efficiency (IQE) from the two LEDs. It can be seen that the highest IQE value from the LED B is larger than that of the LED A, reaching nearly 70 %. The current density corresponding to this peak value is approximately 6 A/cm^2, also exceeding that of the

LED A. Moreover, after reaching their peak values, while the IQE of the LED A is drastically reduced as the current density rises, the IQE of the LED B slowly decreases with the current density.

One reason leading to such a difference might be the lower hole injection into the unshaded parts of the active layer in the LED A. Thus, the charge-carrier profile at the interface between the p-GaN layer and the MQW region was investigated and is shown in Figure 4. This profile is taken at a higher voltage than the one corresponding to the IQE peak value. In such situation, the space-charge-region (SCR) width becomes extremely small and the region's edges move towards the interfaces of the MQW region. The hole concentration at the interface p-layer/MQW can be considered proportional to the hole-current density.

The hole-concentration profile at the interface is represented by the curve, while the parts corresponding to the unshaded areas are marked by the color. They clearly show that the hole concentration in the areas situated right below the cathodes (blank areas) is significantly higher than that in the other areas. This phenomenon can be explained by the fact that the areas shaded by the cathodes benefit from a direct hole-injection under the influence of a strong electric field, whereas in the unshaded areas the injected-hole concentration is only slightly raised by the spreading phenomenon. At this interface, the electric field due to the lattice mismatch between the p-GaN layer and the InGaN quantum well and the spontaneous polarization of GaN altogether hinder the hole injection into the active region. The strong electric field under the shaded area reduces this polarization-induced field better than that in the unshaded areas. This fact also implies that a large part of the luminous intensity is lost because the radiative-recombination must be strongest in those shaded areas.

The average hole concentration in the unshaded areas is higher in the multiple-cathode LED B than in the single-cathode LED A. Indeed, at this interface, the average hole-concentration in the unshaded areas is $1.72 \times 10^{15}\,\mathrm{cm}^{-3}$ in the LED A and $1.23 \times 10^{16}\,\mathrm{cm}^{-3}$ in the LED B, meaning that the hole injection is more efficient in the LED B. Furthermore, the average electric-field intensity in those unshaded parts of the interface is directed towards the p-GaN layer with values of 66 kV/cm and 25 kV/cm in the LED A and the LED B respectively. Consequently, the hole transport is further hampered in the LED A than in the LED B, resulting in a lower hole concentration in the active area.

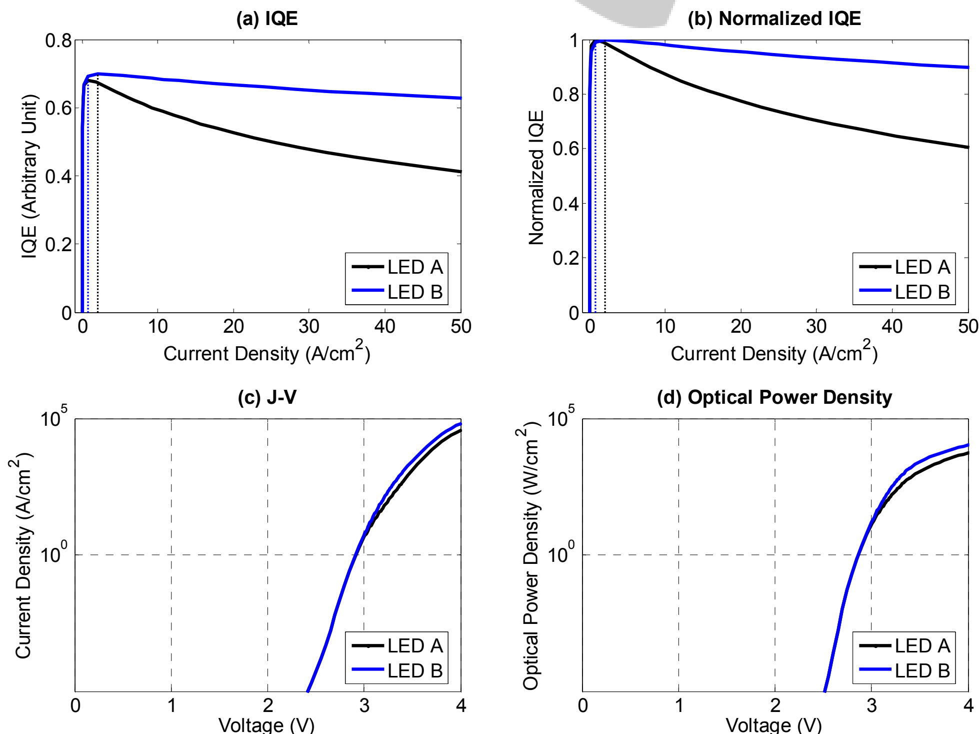

Figure 3: The simulation results from the LED A (black solid line) and the LED B (blue solid line), respectively a) Efficiency, b) Normalized efficiency, c) J-V characteristic curve and d) L-V curve.

SCITEPRESS SCIENCE AND TECHNOLOGY PUBLICATIONS

At the interface between the n-type layer and the MQW region, the electron-concentration profile (not shown here) resembles to the above-mentioned hole-concentration. The average electron-concentrations in the unshaded areas are respectively 0.76×10^{16} cm^{-3} and 2.62×10^{16} cm^{-3} in the LED A and the LED B. However, the average electric-field intensities are approximately equivalent: 5.4×10^5 V/cm in LED A and 5.9×10^5 V/cm in LED B.

The injected-hole concentration in the LED B is more than seven times higher than that in the LED A, while the same ratio for the injected-electron concentration between these LEDs is approximately 3.5. Thus, we suspect that the p-type layer plays a major role in LED current-injection and particularly in balancing the charge ratio. Moreover, as shown by Figure 5, the local injected-electron/injected-hole ratio is much higher in the LED A than in the LED B, even reaching values as high as 45 at the structure's edges. This ratio in the LED B consistently fluctuates at around 2, suggesting that the carrier concentration profile tends towards an equilibrium which may reduce the unbalanced charge-ratio and consequently the carrier leakage. Such values are remarkable as both structures do not have any electron-blocking layer and the ionized-donor concentration in the n-type layer is higher than the ionized-acceptor concentration in the p-type layer. Furthermore, this local ratio increases as the distance from the contact edge increases, while the carrier concentration and the local current-density decrease. This observation implies that in this type of LED structure, the electrode spacing is critical since if it is not well implemented it can induce areas where poor and unbalanced carrier-injection occurs. This problematic should be very critical in the conventional-chip structure where the mesa length must be taken into account during LED design, as remarked by (Huang et al., 2013).

6.4 Overview

Experimental measurements and simulations on LEDs with two different cathode-structures have been realized. The characterization and simulation results show a strong correlation and demonstrate an improvement in the LED internal-quantum-efficiency by optimizing the current injection into the active region. This injection optimization is critical in LED design as it affects the injected-carrier concentration-ratio at the active-region edges and in respect of this ratio variation, the carrier leakage can be either reduced or intensified. The simulations also indicate an important role of the LED p-type-layer in the current injection and, consequently, in the IQE droop. The employment of the multiple-stripe-like cathode-structure slightly varies the electron injection and the electric field from the n-side of the active region, but strongly modulates those from the p-side. These unbalanced injection-induced influences tend to imply a major

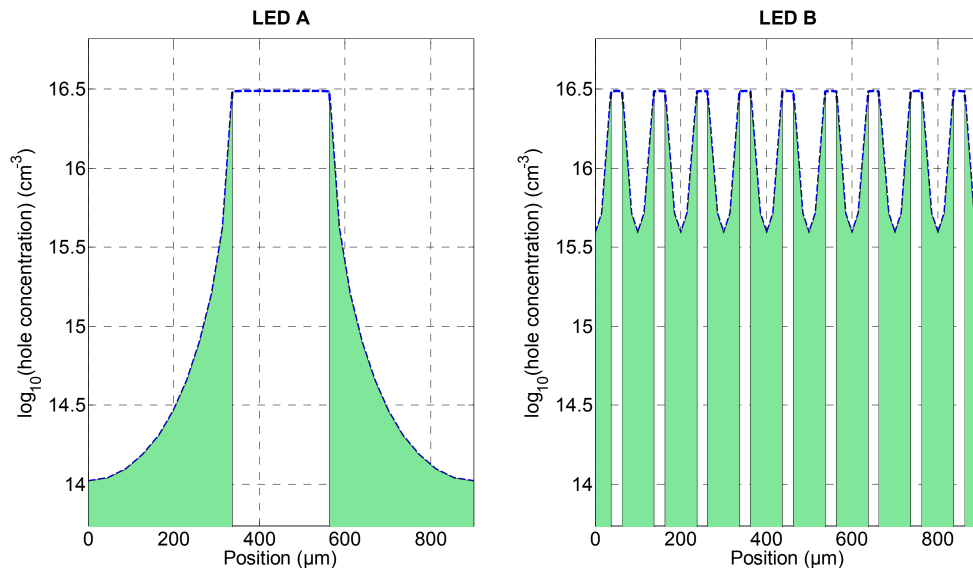

Figure 4: Hole-concentration profile at the p-layer/MQW-region interface (left: LED A, right: LED B) at a voltage higher than that corresponding to the peak IQE value. It implies that the total colored-surface is higher in the LED B than in the LED A.

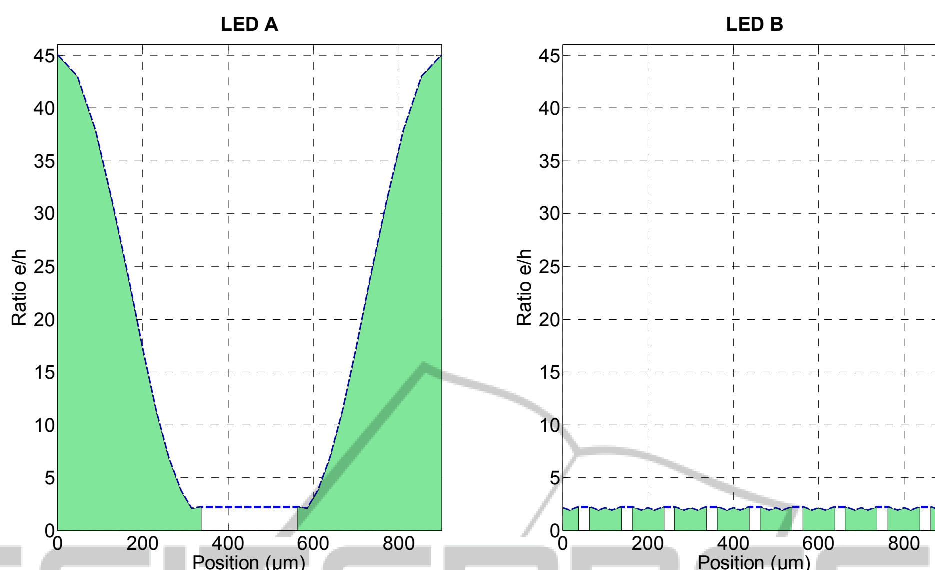

Figure 5: The local injected-electron/injected-hole into the active region at a voltage higher than that corresponding to the peak IQE for the LED A (left) and the LED B (right). The LED A shows a much more unbalanced local-carrier-profile-ratio than the LED B and is seemingly more prone to the carrier leakage.

impact of the carrier leakage and perhaps a lesser role of the Auger-recombination processes in the IQE droop of LEDs without electron-blocking layer. It should be noted that, as stated at the beginning, in the simulations, the SRH carrier-lifetime and the Auger coefficient were intentionally chosen in order for the SRH-recombination rate to be reduced and for the Auger-recombination rate to be amplified. Several recent results (not detailed in this paper) suggested that the IQE curve and peak do not coincide with those of the radiative-recombination-percentage curve. The latter represents the percentage of the radiative-recombination rate in the total recombination rate. In addition to the difference between the electron and hole concentrations at the edges of the active region, this impact from carrier leakage may imply that the commonly-used ABC-model should be applied very carefully to LEDs without any electron-blocking layer as it usually assumes that electron and hole concentrations are equivalent at high injection.

6.5 Perspective

As stated in the previous section, the p-GaN layer may play a major role in the efficiency loss. To further understand the p-type-layer impact on the carrier injection, further experiments are needed to study its carrier transport properties. Those properties are expected to be characterized with respect to the GaN polarity by using several specific sample-designs. Important parameters such as the temperature and the electric field will be varied during the measurements.

Apart from the material characterization, the pulsed electroluminescence will help establish the injected-carrier ratio inside an LED under an electrical excitation. As seen from the simulation results, this ratio is expected to be unbalanced, especially in LEDs without any electron-blocking-layer. The data acquisition is still ongoing and will soon be followed by the data-processing phase.

The obtained results are expected to be communicated soon and contribute to the decorrelation of the IQE components.

ACKNOWLEDGMENT

This PhD. thesis is funded by the optoelectronic department (LETI/DOPT) of CEA Grenoble research center. The author is grateful to the CNRS/CRHEA for the provided samples.

REFERENCES

Bertazzi, F., Goano, M., Zhou, X., Calciati, M., Ghione, G., Matsubara, M., Bellotti, E., 2013. Comment on "Direct Measurement of Auger Electrons Emitted from a Semiconductor Light-Emitting Diode under Electrical Injection: Identification of the Dominant

Mechanism for Efficiency Droop" [Phys. Rev. Lett. 110, 177406 (2013)].

Cabalu, J.S., Thomidis, C., Moustakas, T.D., Riyopoulos, S., Zhou, L., Smith, D.J., 2006. Enhanced internal quantum efficiency and light extraction efficiency from textured GaN/AlGaN quantum wells grown by molecular beam epitaxy. J. Appl. Phys. 99, 064904. doi:10.1063/1.2179120.

Cao, X.A., Arthur, S.D., 2004. High-power and reliable operation of vertical light-emitting diodes on bulk GaN. Appl. Phys. Lett. 85, 3971. doi:10.1063/1.1810631.

David, A., Grundmann, M.J., Kaeding, J.F., Gardner, N.F., Mihopoulos, T.G., Krames, M.R., 2008. Carrier distribution in (0001)InGaN/GaN multiple quantum well light-emitting diodes. Appl. Phys. Lett. 92, 053502. doi:10.1063/1.2839305.

Delaney, K.T., Rinke, P., Van de Walle, C.G., 2009. Auger recombination rates in nitrides from first principles. Appl. Phys. Lett. 94, 191109. doi:10.1063/1.3133359.

Della Sala, F., Di Carlo, A., Lugli, P., Bernardini, F., Fiorentini, V., Scholz, R., Jancu, J.-M., 1999. Free-carrier screening of polarization fields in wurtzite GaN/InGaN laser structures. Appl. Phys. Lett. 74, 2002. doi:10.1063/1.123727.

Galler, B., Drechsel, P., Monnard, R., Rode, P., Stauss, P., Froehlich, S., Bergbauer, W., Binder, M., Sabathil, M., Hahn, B., Wagner, J., 2012. Influence of indium content and temperature on Auger-like recombination in InGaN quantum wells grown on (111) silicon substrates. Appl. Phys. Lett. 101, 131111. doi:10.1063/1.4754688.

Hader, J., Moloney, J.V., Pasenow, B., Koch, S.W., Sabathil, M., Linder, N., Lutgen, S., 2008. On the importance of radiative and Auger losses in GaN-based quantum wells. Appl. Phys. Lett. 92, 261103. doi:10.1063/1.2953543.

Hangleiter, A., Hitzel, F., Netzel, C., Fuhrmann, D., Rossow, U., Ade, G., Hinze, P., 2005. Suppression of Nonradiative Recombination by V-Shaped Pits in GaInN/GaN Quantum Wells Produces a Large Increase in the Light Emission Efficiency. Phys. Rev. Lett. 95. doi:10.1103/PhysRevLett.95.127402.

Huang, S., Fan, B., Chen, Z., Zheng, Z., Luo, H., Wu, Z., Wang, G., Jiang, H., 2013. Lateral Current Spreading Effect on the Efficiency Droop in GaN Based Light-Emitting Diodes. J. Disp. Technol. 9, 266–271. doi:10.1109/JDT.2012.2225092.

Iveland, J., Martinelli, L., Peretti, J., Speck, J.S., Weisbuch, C., 2013. Direct Measurement of Auger Electrons Emitted from a Semiconductor Light-Emitting Diode under Electrical Injection: Identification of the Dominant Mechanism for Efficiency Droop. Phys. Rev. Lett. 110. doi:10.1103/PhysRevLett.110.177406.

Kim, H., Cho, J., Lee, J.W., Yoon, S., Kim, H., Sone, C., Park, Y., Seong, T.-Y., 2007. Measurements of current spreading length and design of GaN-based light emitting diodes. Appl. Phys. Lett. 90, 063510. doi:10.1063/1.2450670.

Kim, M.-H., Schubert, M.F., Dai, Q., Kim, J.K., Schubert, E.F., Piprek, J., Park, Y., 2007. Origin of efficiency droop in GaN-based light-emitting diodes. Appl. Phys. Lett. 91, 183507. doi:10.1063/1.2800290.

Kioupakis, E., Rinke, P., Delaney, K.T., Van de Walle, C.G., 2011. Indirect Auger recombination as a cause of efficiency droop in nitride light-emitting diodes. Appl. Phys. Lett. 98, 161107. doi:10.1063/1.3570656.

Krames, M.R., Christenson, G., Collins, D., Cook, L.W., Craford, M.G., Edwards, A., Fletcher, R.M., Gardner, N.F., Goetz, W.K., Imler, W.R., Johnson, E., Kern, R.S., Khare, R., Kish, F.A., Lowery, C., Ludowise, M.J., Mann, R., Maranowski, M., Maranowski, S.A., Martin, P.S., O'Shea, J., Rudaz, S.L., Steigerwald, D.A., Thompson, J., Wierer, J.J., Yu, J., Basile, D., Chang, Y.-L., Hasnain, G., Heuschen, M., Killeen, K.P., Kocot, C.P., Lester, S., Miller, J.N., Mueller, G.O., Mueller-Mach, R., Rosner, S.J., Schneider, J., Richard P., Takeuchi, T., Tan, T.S., 2000. High-brightness AlGaInN light-emitting diodes. pp. 2–12. doi:10.1117/12.382822.

Krames, M.R., Shchekin, O.B., Mueller-Mach, R., Mueller, G.O., Zhou, L., Harbers, G., Craford, M.G., 2007. Status and Future of High-Power Light-Emitting Diodes for Solid-State Lighting. J. Disp. Technol. 3, 160–175. doi:10.1109/JDT.2007.895339.

Li, C.-K., Wu, Y.-R., 2012. Study on the Current Spreading Effect and Light Extraction Enhancement of Vertical GaN/InGaN LEDs. IEEE Trans. Electron Devices 59, 400–407. doi:10.1109/TED.2011.2176132.

Morkoç, H., 2008. Handbook of nitride semiconductors and devices. Wiley-VCH ; John Wiley, distributor], Weinheim : [Chichester.

Mukai, T., Yamada, M., Nakamura, S., 1999. Characteristics of InGaN-Based UV/Blue/Green/Amber/Red Light-Emitting Diodes. Jpn. J. Appl. Phys. 38, 3976–3981. doi:10.1143/JJAP.38.3976.

Ni, X., Fan, Q., Shimada, R., Özgür, U., Morkoç, H., 2008. Reduction of efficiency droop in InGaN light emitting diodes by coupled quantum wells. Appl. Phys. Lett. 93, 171113. doi:10.1063/1.3012388.

Piprek, J., Farrell, R., DenBaars, S., Nakamura, S., 2006. Effects of built-in polarization on InGaN-GaN vertical-cavity surface-emitting lasers. IEEE Photonics Technol. Lett. 18, 7–9. doi:10.1109/LPT.2005.860045.

Romanowski, Z., Kempisty, P., Sakowski, K., Strąk, P., Krukowski, S., 2010. Density Functional Theory (DFT) Simulations and Polarization Analysis of the Electric Field in InN/GaN Multiple Quantum Wells (MQWs). J. Phys. Chem. C 114, 14410–14416. doi:10.1021/jp104438y.

Rozhansky, I.V., Zakheim, D.A., 2007. Analysis of processes limiting quantum efficiency of AlGaInN LEDs at high pumping. Phys. Status Solidi A 204, 227–230. doi:10.1002/pssa.200673567.

Schubert, M.F., Chhajed, S., Kim, J.K., Schubert, E.F.,

Koleske, D.D., Crawford, M.H., Lee, S.R., Fischer, A.J., Thaler, G., Banas, M.A., 2007. Effect of dislocation density on efficiency droop in GaInN⁄GaN light-emitting diodes. Appl. Phys. Lett. 91, 231114. doi:10.1063/1.2822442.

Schubert, M.F., Xu, J., Kim, J.K., Schubert, E.F., Kim, M.H., Yoon, S., Lee, S.M., Sone, C., Sakong, T., Park, Y., 2008. Polarization-matched GaInN⁄AlGaInN multi-quantum-well light-emitting diodes with reduced efficiency droop. Appl. Phys. Lett. 93, 041102. doi:10.1063/1.2963029.

Son, J.H., Kim, B.J., Ryu, C.J., Song, Y.H., Lee, H.K., Choi, J.W., Lee, J.-L., 2012. Enhancement of wall-plug efficiency in vertical InGaN/GaN LEDs by improved current spreading. Opt. Express 20, A287. doi:10.1364/OE.20.00A287.

Thompson, G.H.B., 1980. Physics of semiconductor laser devices. J. Wiley, Chichester [Eng.] ; New York.

Turin, V.O., 2005. A modified transferred-electron high-field mobility model for GaN devices simulation. Solid-State Electron. 49, 1678–1682. doi:10.1016/j.sse.2005.09.002.

Xu, J., Schubert, M.F., Noemaun, A.N., Zhu, D., Kim, J.K., Schubert, E.F., Kim, M.H., Chung, H.J., Yoon, S., Sone, C., Park, Y., 2009. Reduction in efficiency droop, forward voltage, ideality factor, and wavelength shift in polarization-matched GaInN/GaInN multi-quantum-well light-emitting diodes. Appl. Phys. Lett. 94, 011113. doi:10.1063/1.3058687.

Zhang, Z.-H., Ju, Z., Liu, W., Tan, S.T., Ji, Y., Kyaw, Z., Zhang, X., Hasanov, N., Sun, X.W., Demir, H.V., 2014. Improving hole injection efficiency by manipulating the hole transport mechanism through p-type electron blocking layer engineering. Opt. Lett. 39, 2483. doi:10.1364/OL.39.002483.

SCITEPRESS SCIENCE AND TECHNOLOGY PUBLICATIONS